LIQUEFACTION POTENTIAL IN CHIANG RAI PROVINCE, NORTHERN THAILAND DUE TO 6.8 M_W EARTHQUAKE ON MARCH 24, 2011

Lindung Zalbuin MASE[1], Tetsuo TOBITA[2] and Suched LIKITLERSUANG[3]

[1]Doctoral Student, Faculty of Engineering, Dept. of Civil Eng., Chulalongkorn University
(254 Phayathai Rd, Pathumwan, Bangkok 10330, Thailand)
E-mail:lindung.za@student.chula.ac.th
[2]Member of JSCE, Associate Professor, Dept. of Civil, Environmental, and Applied System Eng., Kansai University
(3-3-35 Yamate-cho, Suita, Osaka 564-8680, Japan)
E-mail:tobita@kansai-u.ac.jp
[3]Professor, Faculty of Engineering, Dept. of Civil Eng., Chulalongkorn University
(254 Phayathai Rd, Pathumwan, Bangkok 10330, Thailand)
E-mail:fceslk@eng.chula.ac.th

Liquefaction potential in Chiang Rai Provice in Northern Thailand is investigated with data obtained after the 6.8 M_w earthquake on March 24, 2011. Several investigation data were collected and used to perform one dimensional wave propagation analysis by using non-linear finite element method, based on 0.206 g as the maximum acceleration recorded for input motion in Chiang Rai area. Furthermore, input motion was applied at bottom of soil column to observe soil behavior under seismic loading of considered earthquake.The result shows that liquefaction potentially could occur at shallow depth, which is also followed by settlement due to compressibility of soil due to earthquake shaking. Moreover, the liquefaction duration at shallower depth is longer than deeper depth, which may be caused by the effect of fines content and bottom-up pressure of wave propagation energy triggering the pore water pressure concentrated at shallower depth.

Key Words : *liquefaction potential, non-linear finite element, seismic response analysis, tarlay earthquake, earthquake shaking*

1. INTRODUCTION

On 24th of March 2011, people lived near border of Thailand-Myanmar-and Laos were shocked by the earthquake shaking with magnitude of 6.8 M_w which hit that area. The epicenter of this earthquake was reported at Tarlay, Myanmar, with focal depth of 10 km, which triggered by the activity of Nam-Ma Fault.

Northern Thailand was one of the impacted areas due to Tarlay Earthquake. Many damages of structure and infrastructure were found in this area, especially Chiang Rai, the closest Province in Thailand to the earthquake epicenter (about 33 km). It was known that PGA (peak ground acceleration) of earthquake recorded at Mae Sai Station (in Chiang Rai Province) was 0.206g. The energy of earthquake in term of PGA had shown not only the structure damages but also the other catastrophic hazard, such as liquefaction (shown in Figure 1). Learning from this first liquefaction event, the intensive studies of soil liquefaction in Thailand has been started to be conducted.

Several researchers reported and studied the liquefaction event due to Tarlay earthquake. Ruangrassamee et al.[1] also reported the liquefaction damages due to the earthquake. Based on their observation, sand layer with loose to medium density were liquefied during 2011 earthquake. These sand layer are generally present at top layers in Chiang Rai and Chiang Mai Province.

Soralump and Feugaugsorn[2] reported that Mae Sai District was the vulnerable area of liquefaction due to Tarlay earthquake. Similar to Ruangrassamee report, they concluded that it might be liquefied from medium to loose sand layer at depth of 3.5 to 11 m. They also reported the liquefaction found on this area was the first eyewitness in Thailand during modern term of Thailand. Furthermore, Tanapalungkorn and Teachavorasinskun[3] conducted the study of liquefaction susceptibility in Northern Thailand by considering 2011 earthquake. In their study, they also confirmed that Northern Part of Thailand especially Chiang Rai was vulnerable to undergo liquefaction. Mase et al.[4] reviewed previous study of liquefaction in Northern Thailand due to Tarlay earthquake. In their study, they used empirical approach to analyze liquefaction potential in Chiang Rai area. Based on their study, they also concluded and confirmed that liquefaction had potential to occur.

Fig.1-a Liquefaction evidences on free field due to Tarlay Earthquake (Ruangrassamee et al.[1])

Fig.1-b Liquefaction evidences on paddy field due to Tarlay Earthquake (Tapanalungkorn and Teachavorasinskun.[3])

Referring to previous studies, in general, most previous studies of liquefaction in Northern Part of Thailand were conducted based on the site investigation combined with empirical approach to analyze the critical depth of liquefaction. However, the detail study in term of soil behavior under dynamic load corresponding to the related actual earthquake (Tarlay earthquake ground motion) is still rare to be conducted. Therefore, a study of non-linear finite element analysis based on effective stress model is conducted, especially in Chiang Rai Area. This intensive study of soil liquefaction associated with seismic behavior of soil is very important to be conducted to observe soil liquefaction in detail.

2. METHODOLOGY

(1) Research area and its geological condition

This study was focused on Chiang Rai. There are three site investigation points studied in research area, which is show in Figure 2. In this study, site investigation was focused on three locations, i.e. Wiang Pa Pao (CR-1), Muang (CR-2) and Mae Sai (CR-3) districts. Through to site investigation points, SPT and SASW data were collected.

Furthermore, the desk study was also conducted to interpret the sub-soils condition based on the collected data. Example of soil investigation test conducted in Chiang Rai is presented in Figure 3. According to desk study, Chiang Rai sub-soils were dominated by sandy soils, which were classified as SP, SM, and SC with FC of 10 to 26%. Nevertheless, clayey soil with thin layer was also found on some boreholes. In general, ground water table on each site was found on very shallow depth, about 0 to 2.8 m deep.

The distribution of $(N_1)_{60}$ in this area ranged from 3 to 25 blows/feet, whereas the range of V_{S30} was 285 m/s to 319 m/s. The value of V_{S30} was also used in determining the site class of investigation area, especially based on National Earthquake Hazards Reduction Program or NEHRPcriteria[5]. According to this criteria, the general site class of Chiang Rai was categorized as Site Class Type D (Very Stiff Soil).

(2) Ground motion

To model wave propagation under existing wave of Tarlay Earthquake, a recorded ground motion was applied at each base of site investigation point. Ground motion selected in this study was ground motion recorded at Mae Sai station (the closest station to Tarlay earthquake epicenter), which was obtained from Thai Meteorological Department (TMD) in 2015[6]. The interpretation of time history and propagating acceleration used in this study is presented in Figure 4. Based on Figure 4, it can be seen that maximum peak ground acceleration resulted is 0.206g. Moreover, the ground motion record also shows that in 10^{th} to 30^{th} seconds of seismic motion can be categorized as the significant duration of this earthquake. The impact of this wave motion will be discussed in this paper.

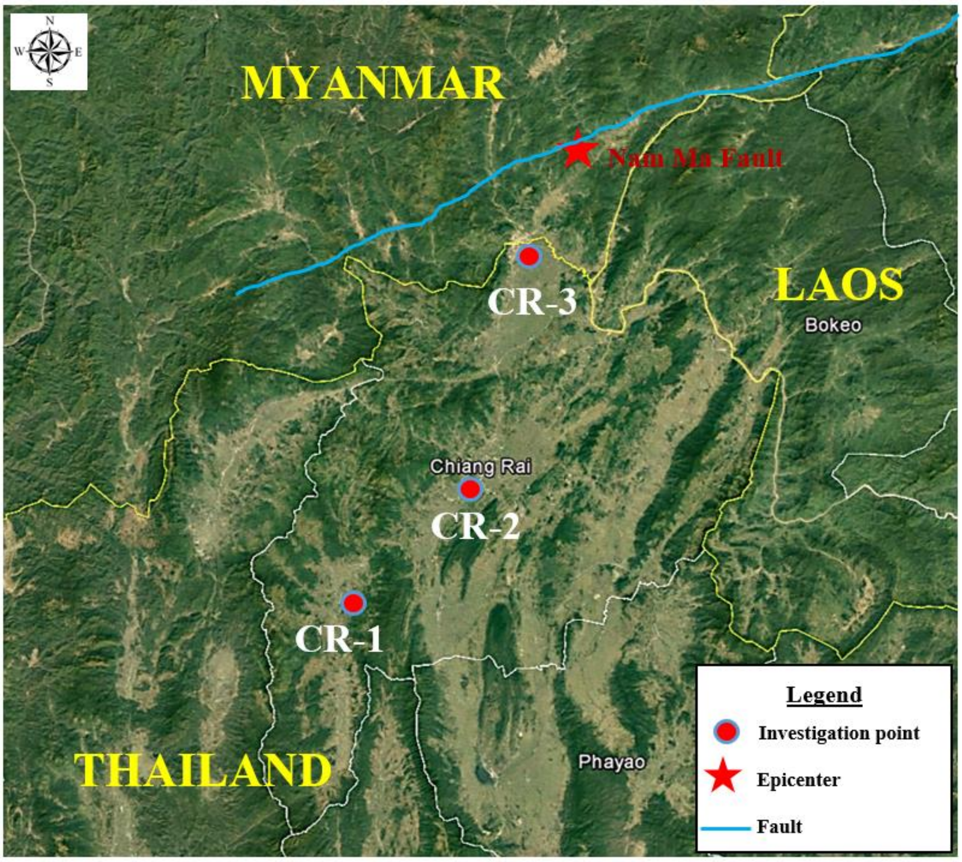

Fig.2 Location of site investigation points conducted in this study and the epicenter location of 6.8 M_w on March 24, 2011 in Tarlay

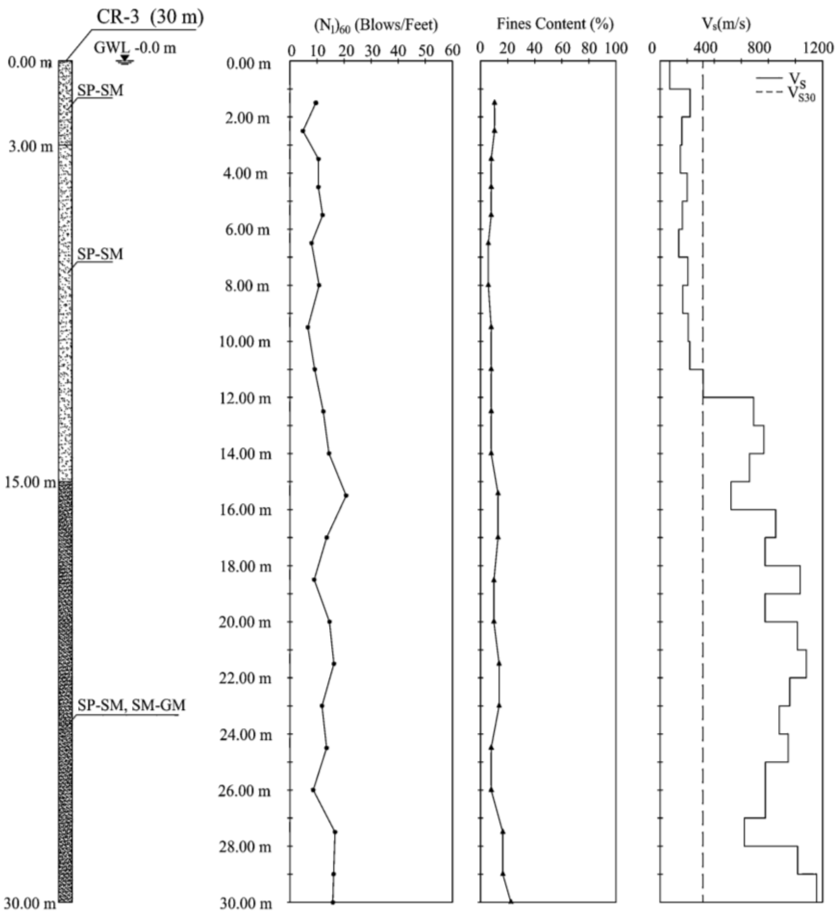

Fig.3 Example of site investigation conducted in Chiang Rai Province

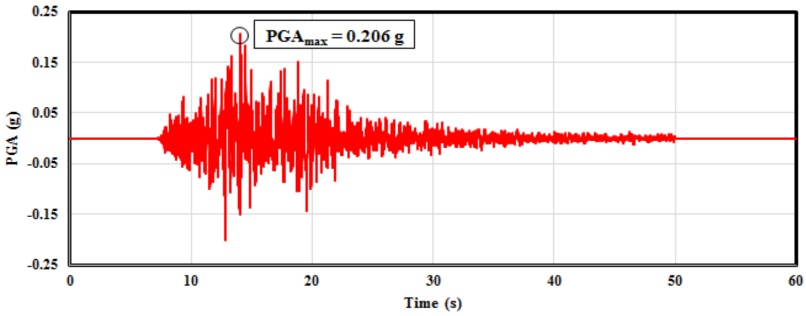

Fig.4 Acceleration record and its spectral acceleration recoreded Mae Sai Station (Northern Thailand) on 24 March 2011[6)]

(3) One-dimensional finite element approach of seismic response analysis

In this study, soil liquefaction behavior subjected to Tarlay earthquake is observed by occupying non-linear finite element effective stress model proposed by Elgamal et al.[7)]. In this method, non-linearity of soil is simulated by using incremental plasticity to model permanent deformation and hysteretic damping as well. The finite element approach in both dry and saturated strata used the coupled solid-fluid approach. Therefore, this method is able to generate and dissipate excess pore water pressure as well. Moreover, in its computational process, this approach may explore some important information related to seismic response of soil and soil behavior under dynamic load. The brief explanation about constitutive modelling and theory of this approach is discussed here.

It has been known, where the cyclic stress-strain behavior of saturated sandy soil is very complex and not simple[8)]. However, there is any exception for very loose sands at very low confining pressure, which behave as contractive material, indicating generation of positive pore water pressure. Ishihara et al.[9)] explained this phenomena, which is now called as phase transformation (PT) line as the better understanding to describe contractive-dilative behavior of saturated sand. The general trend of cyclic effective stress path and shear-strain curves to explain Ishihara et al.[9)] explanation is presented in Figure 5. Once at value of the shear stress ratio has been reached, then there is transformation phase from contractive to dilative behavior. This condition happens when effective stress path achieves phase transformation line (phase 1) and it will be attributed by the increment of soil stiffness and change of movement of effective stress path to the right side (phase 2). Once the loading is reversely applied from compression to extension, the decrease of effective confining pressure happens and soil behaves as contractive phase (phase 3 to phase 4), and it may failure at phase 6. The reverse of compression to extension will reach the transformation line at phase 7, result in an accumulation of shear strain (phase 8). As the result, it is possible to failure at phase 9. For this cyclic, accumulation of excess pore water pressure exists, but after the phase transformation is moved to accumulation decrease level, e.g. at phases 4-5 and phases 7-8.

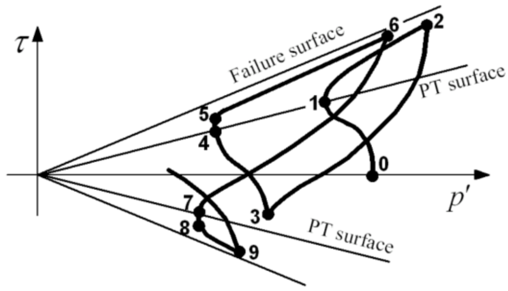

Fig.5-a Effective stress path of shear strain model for sand under cyclic mobility[10)]

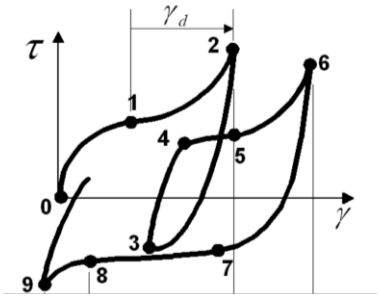

Fig.5-b Mean principal effective stress; τ, shear stress; γ, shear strain, and PT, phase transformation locus of sand under cyclic mobility[10)]

Corresponding to cyclic mobility illustrated in Figure 5, some constitutive modellings of cyclic mobility were developed. One of them is non-linear finite element effective stress, which is able to answer the problem of cyclic mobility such as liquefaction. Constitutive modelling of soil liquefaction used in non-linear finite element effective stress model proposed by Elgamal et al.[7)] is developed based on Parra[11)] and Yang[12)], in which are based on framework of multi-yield surface plasticity proposed by Prevost[13)].

In this model, emphasis is on controlling magnitude of cycle by cycle permanent shear strain accumulation in several sand types[11) 12)]. Moreover, the complex phases including contractive, perfectly plastic, and dilative phases is incorporated by the flow rule, which is able to significantly change the characteristic model response for reproducing the salient cyclic mobility mechanism and exercising more direct control over shear strain accumulation[10]. In addition, since this model follows the multi-yield surface, then a new kinematic hardening rule is developed, as illustrated in Figure 6.

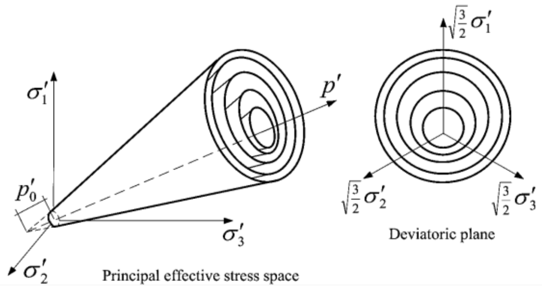

Fig.6 Multi-yield surface of kinematic hardening yield locus in principal stress and deviatoric plane (after Prevost[13] Parra[11] and Yang[12])

Since a new kinematic hardening rule is developed into multi-yield surface, then the stiffness is evaluated in each incremental step for each single element. In addition, in calculation of finite element, the excess of water pressure and water pressure dissipation are capable of modelling in this model under cyclic loading, either if the permeability is large or if the loading frequency is relatively small. The detail explanation of the constitutive model used in non-linear finite element approach can be found on Elgamal et al.[14], Yang and Elgamal[15], Elgamal et al.[10], Yang et al.[16] and Yang et al.[17].

(4) Modeling criteria

One-dimensional non-linear finite element effective stress is occupied in this study subjected to the considered soil column based on site investigation result. The soil column is assumed to be fully saturated condition. It is taken to consider the worst condition of soil column. The initial vertical effective stress is estimated based on water table and soil density, whereas initial lateral effective stress is estimated based on the calculation of initial effective stress and coefficient of lateral earth pressure at rest (K_o). The value of initial vertical effective stress is then used to estimate excess pore water pressure ratio (r_u) to predict if liquefaction occurs or not. In this study, seismic response analysis and liquefaction observation is applied by propagating the input motion (Mae Sai ground motion) through to soil column divided into elements. The illustration of soil column model and wave propagation mechanism is presented in Figure 7. As shown in Figure 7, it can be seen that boundary condition is limited only for the soil column on vertical direction. However, displacement in both vertical and horizontal directions could be happened during wave propagation. Once the wave is propagated from the base of soil column, the water pressure will build up only in vertical direction. It is caused by no drainage in lateral direction of element boundaries. The soil column is underlain by elastic half space, which is impermeable or no drainage path.

Pender et al.[8] who studied the effect of permeability on the cyclic generation and dissipation of pore pressures in saturated gravel layers in Christchurch, New Zealand, revealed that there was no any particular sensitivity to the fineness of element subdivision, when observed the 10 m soil column divided into 10, 20, 30, 40, and 80. Therefore in the computations of their study, 0.5 m thick elements was selected. In this study, mesh size is determined from the relationship between V_s and frequency ($V_s=\lambda.f$) for V_s minimum obtained per 1 m of measurement to derive d mesh for overall depth. The derivation of d mesh is also described in Figure 7. Material properties of each layer shown is determined based on either undisturbed or disturbed sampling test from the soil sample taken from boring test. Parameters needed in analysis include soil density (γ), soil cohesion (c), internal friction angle (ϕ), permeability, shear wave velocity (V_s) effective confinement reference ($p'\,ref$), coefficient of lateral earth pressure (K_o), permeability (k), pea shear strain (γ_{max}), liquefaction parameter, and Contractive-Dilative Parameters. The guidance in determining the input parameters for this method was presented in Elgamal et al.[7]. The data obtained is then used in simulation to achieve the description of liquefaction potential on each sites. The input material on each layer of boreholes is listed in Table 1.

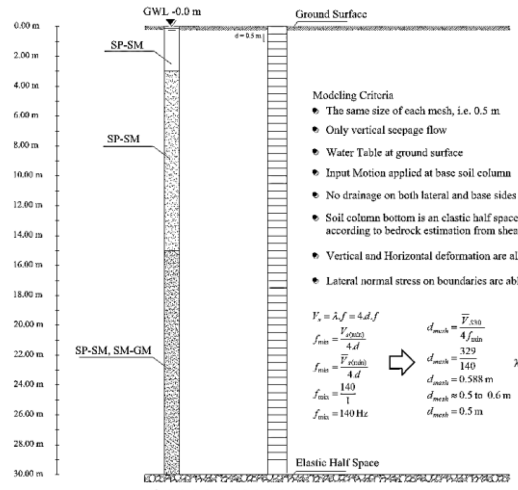

Fig.7 Modeling criteria in this study

Table 1 Input material in this study.

BH	Material	Thickness	γ	*c*	ϕ	FC	permeability (*k*)	*Vs*	*Ko*	*p' ref*	γ_{max}	Liq parameter	Contraction Parameter		Dilation Parameter	
		(m)	(kN/m3)	(kPa)	(°)	(%)	(m/s)	(m/s)	(-)	(kPa)	(%)	*Liq 1*	*c1*	*c2*	*d1*	*d2*
CR-1	CL	2.00	1.30	18.00	-	80	1.10E-09	99	0.67	50	5	-	-	-	-	-
	SP-SM	3.00	1.70	0.30	28	8	6.60E-05	237	0.53	80	5	0.025	0.300	0.200	0.000	10
	SP-SM	5.50	2.00	0.30	29	8	6.60E-05	421	0.52	80	5	0.010	0.060	0.500	0.400	10
	SM, SP-SM, SM-GM	19.50	2.10	0.30	30	11.13	6.60E-05	472	0.50	80	5	0.003	0.010	0.600	0.600	10
CR-2	SP-SM	9.00	1.70	0.30	0	21	6.60E-05	195	1.00	80	5	0.025	0.300	0.200	0.000	10
	SP-SM	7.50	1.70	0.30	29	26	6.40E-05	259	0.52	80	5	0.025	0.300	0.200	0.000	10
	SM-GM,GP	2.50	2.00	0.30	9	19	6.60E-05	266	0.84	80	5	0.010	0.060	0.500	0.400	10
	SC	1.50	2.00	3.00	29	18	6.70E-05	273	0.52	80	5	0.010	0.060	0.500	0.400	10
	SM	3.00	2.00	0.50	19	16	6.90E-05	600	0.67	80	5	0.010	0.060	0.500	0.400	10
	SC	6.00	2.00	3.00	30	21	7.10E-05	634	0.50	80	5	0.010	0.060	0.500	0.400	10
	CL	0.50	1.40	20.00	-	94	1.10E-09	728	0.68	50	5	-	-	-	-	-
CR-3	SP-SM	3.00	1.70	0.30	28	7	6.60E-05	140	0.53	80	5	0.025	0.300	0.200	0.000	10
	SP-SM	12.00	2.00	0.32	29	9	6.90E-05	324	0.52	80	5	0.010	0.060	0.500	0.400	10
	SP-SM,SM-GM	15.00	2.10	0.25	30	9	7.20E-05	736	0.50	80	5	0.003	0.010	0.600	0.600	10

3. RESULT AND DISCUSSION

(1) Pore water pressure and settlement due to liquefaction

Figure 11 is the interpretation of pore water pressure and settlement due to liquefaction corresponding to analyzed depth for Chiang Rai site. For CR-1, excess pore water pressure results in liquefaction from 2 to 5 m deep (SC-SM layer). At this depth, the excess pore water pressure ratio (r_u) resulted is 0.998 to 1.13. for depth of 0 to 2 m, CL layer, liquefaction, excess pore water pressure is still able to exceed the initial effective stress, whereas for depth of 5 to 10.5 m deep (SP-SM layer) and 10.5 to 30 m deep (SM, GP, GM layer), the excess pore water pressure is also unable to trigger liquefaction. After shaking, the dissipated excess pore water pressure is also observed. In general, there is drained pore water pressure occurring, especially in liquefiable layer (2 to 5 m deep). The residual excess pore water pressure seems to be concentrated at this depth range. However, below that depth, pore water pressure is well dissipated, especially at SP-SM layer. These liquefaction phenomena also resulted in the ground settlement. It can be seen settlement up to 1.8 cm occurred at ground surface. It is caused by the compressed sandy layer at 2 to 5 m deep. Meanwhile, for depth of 5 to 30 m deep, the settlement is very small.

For CR-2, liquefaction occurs at depth of 0 to 16.5 m deep (SP-SP in layer 1 and layer 2). It is confirmed by the excess pore water pressure exceeding the initial effective stress on the considered depth. On this depth range, the calculated r_u is 0.971 to 1.06. For layers underneath liquefiable layers, the excess pore water pressure is not strong enough to trigger liquefaction, where the excess pore water pressure ratio resulted is in range of 0.1 to 0.5. Similar to CR-1, the dissipated pore water pressure is also observed. In general, there is no significant dissipated pore water pressure on each depth, except on depth of 4 to 9 m deep. In term of settlement due to compressed liquefiable soil, it can be seen that the settlement at ground surface reaches to 4.15 cm, whereas for the depth of 16.5 to 30 m, the settlement resulted is very small. In general, it can be concluded that the impacted depth of CR-2 is larger than CR-1.

Liquefaction on shallow depth is also found on CR-3. The excess pore water exceeds the initial effective stress at depth of 0 to 15 m deep, which dominated by SP-SM in layer 1 and layer 2. The excess pore water pressure ratio in this range is 0.990 to 1.020. Similar to both previous sites, liquefaction is also not found on deeper depth (from 15 to 30 m deep). In this range, the excess pore water pressure ratio is 0.402 to 0.913. Moreover, dissipated pore water pressure after earthquake shaking reveals that significant dissipated pore water pressure is found on 9.5 m to 21 m deep, whereas for depth of 21 m deep to 30 m deep, there is no pore water pressure dissipated, as well as at depth of 0 to 9.5 m deep. The earthquake shaking is not only trigger the excess pore water pressure induced liquefaction but also trigger settlement induced by liquefiable layers. In CR-3, the settlement at ground surface is observed at 3.15 m deep. This is caused by the accumulation of settlement due to compressed liquefiable layer. Obviously, the significant settlement is measured at ground surface to 15.5 m deep. Meanwhile, at depth of 15.5 to 30 m, the settlement is very small.

In general, from the result of liquefaction analysis based on seismic response analysis, it can be concluded that CR-1 has the lowest potential to undergo liquefaction compared to CR-2 and CR-3. It is confirmed by the existence of susceptible layers, where CR-1 has the susceptible layer about 3 m, and has the impacted of settlement of 1.8 cm obviously observed at ground surface. Meanwhile, between CR-2 and CR-3, the more susceptible site can be determined to CR-2, which has 16.5 m deep susceptible layer, whereas CR-3 has 15.5 m deep. The settlement after liquefaction resulted is also shown that the settlement depth of CR-2 is still larger than CR-3, i.e. 4.15 m and 3.15 m at ground surface for CR-2 and CR-3, respectively.

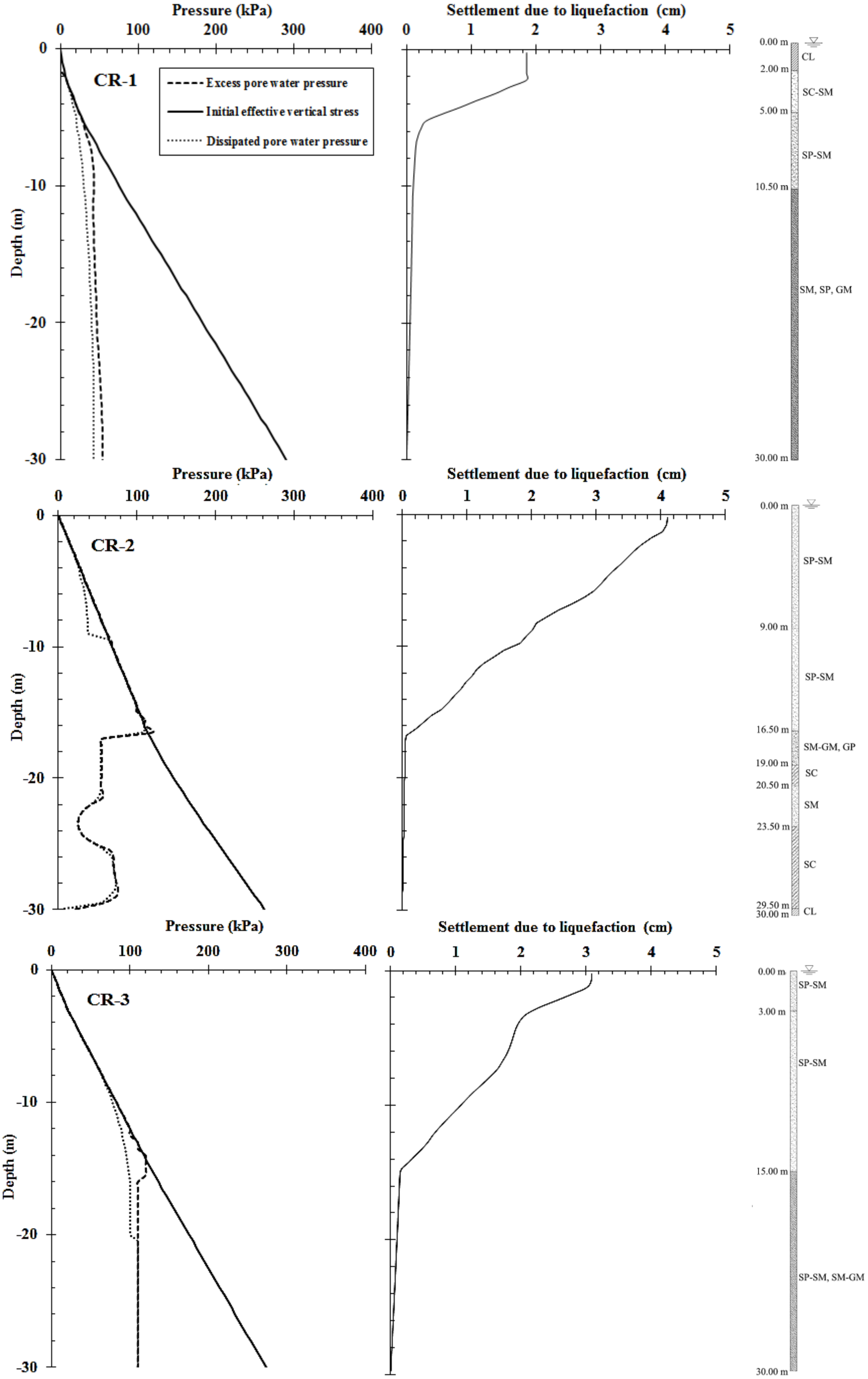

Fig 11. Excess and dissipated pore water pressure on each depth in Chiang Rai Site

(2) Soil layer behavior under wave propagation

The interpretation of soil behavior in liquefiabled layer (at mid thickness) in CR-1, CR-2, and CR-3 are presented in Figure 12. 13, and 14, respectively.

For CR-1, at depth of 1 m (CL layer), excess pore water pressure builds up in small value. At this depth, the shear stress-shear strain is unseen clearly, as well as the effective confinement pressure-shear strain curve. It indicates that seismic loading doesn't give much effect to the excess pore water pressure in this layer. At depth of 2.5 dominated by SP-SP layers, it can be observed that excess pore water pressure has exceeded the initial effective stress at 9th seconds, remain constant reaching the initial effective stress up to 1 minutes. It seems that after shaking pore pressure is not easily drained. The non-linear behavior also presented in curve of shear strain-shear stress, which show the irregular shape of curve. Meanwhile, the liquefaction phenomenon is also confirmed by the decrease of effective confinement pressure to zero at zero shear strain. This indicates that soil layer loses the shear stress due to effective stress reduction caused by the excess pore water pressure. For the depth of 8 and 22.5 m, the excess pore water pressure generates in maximum value under the initial effective stress. These indicates that the liquefaction doesn't happen. The curve of shear strain-shear stress of both depths also show the linear behavior. It confirms that there is no significant cyclic mobility effecting the soil element. Meanwhile, the effective confinement pressures- shear stress also present that there is no the significant shear stress reduction due to the excess pore water pressure. It can be seen from the figure, that at those depths, shear stress doesn't reach the lowest value as well as the effective confinement pressure.

Generally in CR-2, liquefaction occurs at shallow depth, i.e. from 0 to 16.5 m deep. This result has been confirmed based on the soil behavior on each mid depth of soil layers. At depth of 4.5 m, it can be seen that initial effective stress has been passed by the excess pore water pressure in a short time i.e. 12th s, whereas at depth of 13 m the same phenomena is shown as well. The soil type of these points is dominated by SP-SM. At any depth, i.e. 18 m, 20 m deep, 22 m deep, 26.5 m deep, and 29.75 m deep, the excess pore water pressures are not strong enough to trigger liquefaction. The trend of non-linear behavior is also observed at those liquefiable soils, especially in curve of shear stress-shear strain. In addition, the increase of pore water pressure also causes the effective stress reduction, which resulted in the loss of shear stress. It was obviously seen in shear stress and effective confinement curve. For any other depths, the soil behaviors are likely linear. It seems that there is no significant effect of vibration to generate much excess pore water pressure. Likewise, since the effective confinement pressure increases with depth, then the shear stress increases as well. In other word, to generate liquefaction, the excess pore water pressure required must be larger. It is clearly observed that the effective confinement pressure of non-liquefiable layers does not reach zero.

Similar to both previous sites, liquefaction in CR-3 is also predicted occurring at shallow depth. This estimation can be confirmed by investigating the soil behavior on mid-point of each layer. The liquefiable layers are represented by depth of 1.5 m and 9 m. It is seen that at both points, the excess pore water pressure has exceeded the initial effective stress in short time during vibration, i.e. 9th seconds and 13th seconds. at these points, the shear stress-shear strain behavior also performs the non-linear behavior. It confirms that cyclic mobility occurring at the layers. In addition, the cyclic mobility also drops the effective confinement pressure to be zero. It explains that there is significant excess pore water pressure triggering loss of shear stress at both layers. At depth of 23.5 cm, the excess pore water pressure is still lower than initial effective stress. It shows that the liquefaction event doesn't occur at this layers. It is also confirmed by the linear trend of shear stress-shear strain under cyclic mobility. The effective confinement pressure also doesn't reach zero. It shows that increase of pore pressure is not strong enough to decrease shear stress up to zero and trigger liquefaction.

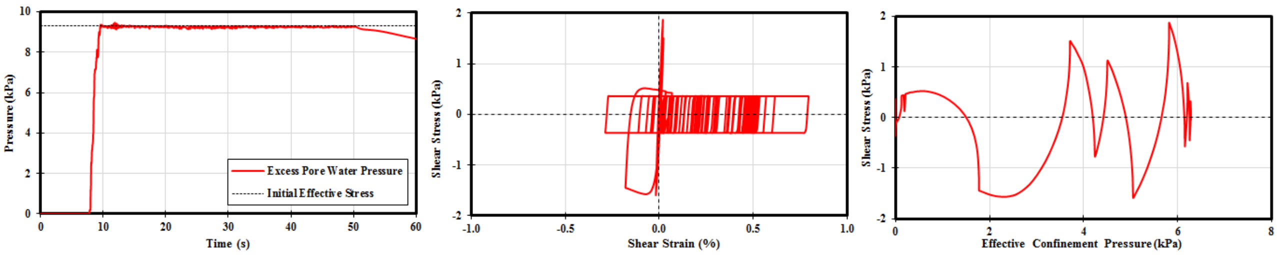

Fig 12. Excess pore pressure vs time, shear strain-shear stress, and effective confinement pressure-shear stress for CR-1 (at 2.5 m)

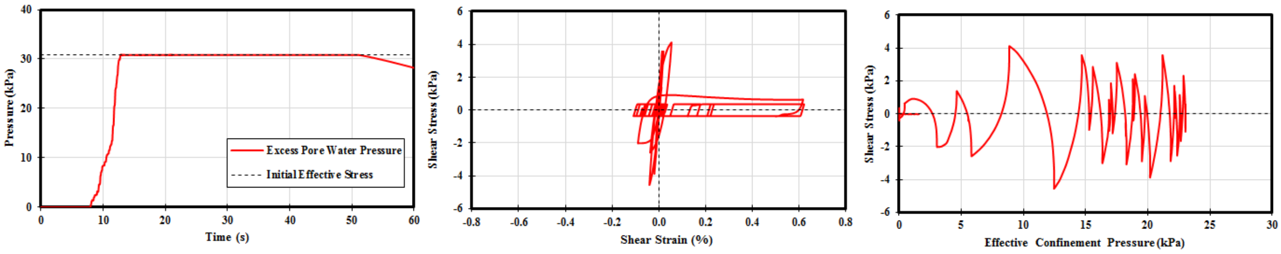

Fig 13a. Excess pore pressure vs time, shear strain-shear stress, and effective confinement pressure-shear stress for CR-2 (at 4.5 m)

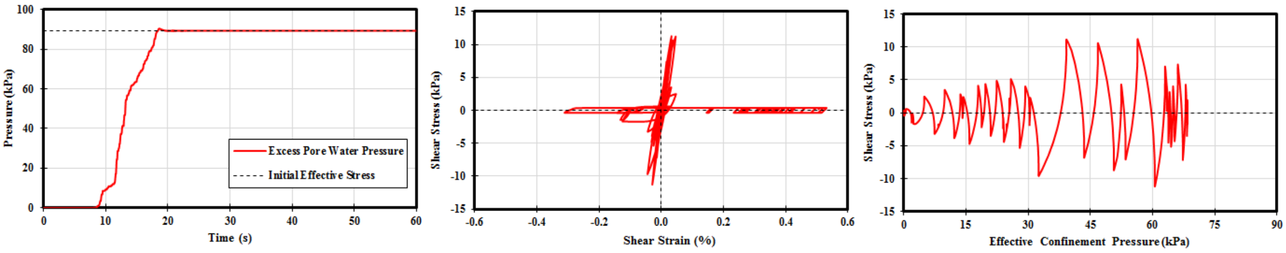

Fig 13b. Excess pore pressure vs time, shear strain-shear stress, and effective confinement pressure-shear stress for CR-2 (at 13 m)

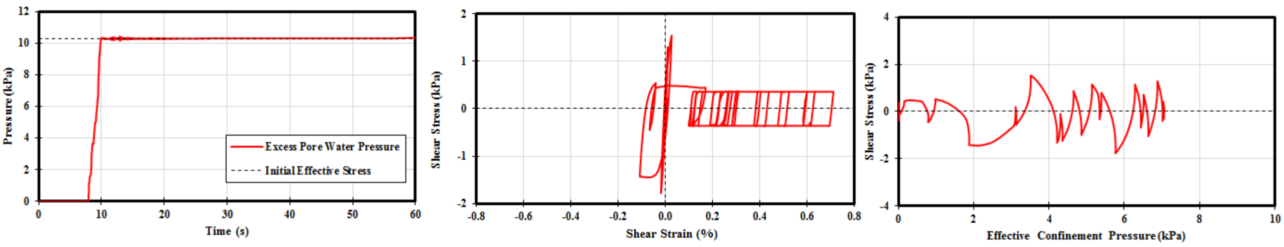

Fig 14a. Excess pore pressure vs time, shear strain-shear stress, and effective confinement pressure-shear stress for CR-3 (at 1.5 m)

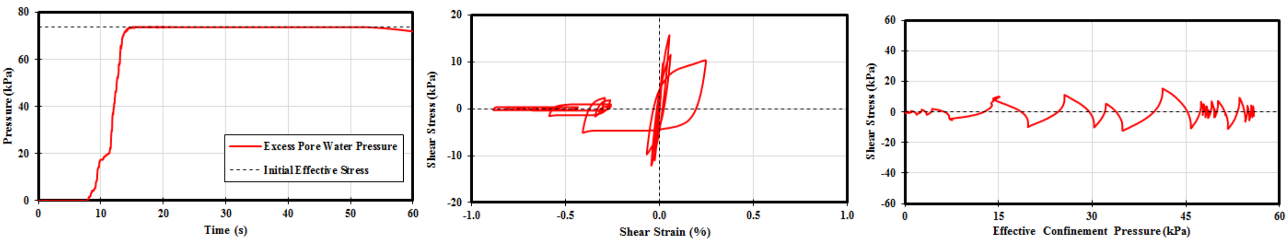

Fig 14b. Excess pore pressure vs time, shear strain-shear stress, and effective confinement pressure-shear stress for CR-3 (at 13 m)

(3) Maximum-minimum excess pore water pressure ratio

Cyclic mobility due to propagating wave caused the saturated sandy soil tends to be denser. However, the cyclic mobility also gives the effect to the soil, i.e. excess pore water pressure and reduction of available stress of soil itself. Cyclic mobility also causes soil behaves dilative after passing phase transformation line. At this point, there is increases of soil stiffness followed by the vertical deformation, which causes the volume change (extension stage). Both volume change and the extension of soil grains will determine the rate of excess pore water pressure. If excess pore water pressure builds up to the same rate of initial effective stress, then liquefaction will occur.

As presented in the previous part, it can be concluded that Chiang Rai site was indicated to undergo liquefaction. In general, the liquefiable layer found in Chiang Rai site is dominated by sandy soil, with soil classification of SP-SM, with $(N_1)_{60}$ of less than 10 blows/ft. Figure 15 shows the comparison of maximum and minimum excess pore water pressure ration in liquefiable layers during shaking and after shaking. The maximum excess pore water pressure of both during shaking and after shaking also do not show the significant difference. It means that after shaking, the maximum excess pore water pressure still concentrates at peak value. In other word, the dissipation of excess pore water pressure is very small. Meanwhile, for minimum excess pore water pressure, it can be seen that there is any difference between excess pore water pressure ratio during and after shaking. It indicates that excess pore water pressure undergoes the dissipation.

In general, maximum excess pore water pressure ratio (Figure 15a) is generated at shallower depth, whereas minimum excess pore water pressure ratio (Figure 15b) is generated at deeper depth. It is actually effected by the excess pore water pressure rate. At shallow depth, due to the bottom-up pressure of excess pore water, the propagated energy transfers the pore water pressure from deeper depth to shallower depth to drain at free surface. In other word, much more pore-pressure needs to be released. As the result, and it will be accumulated and concentrated at shallow depth. The accumulation is obviously decreased the initial effective vertical stress at shallower depth, which is smaller than the deeper depth. Therefore, near ground surface the excess pore water pressure ratio is higher than deeper depth.

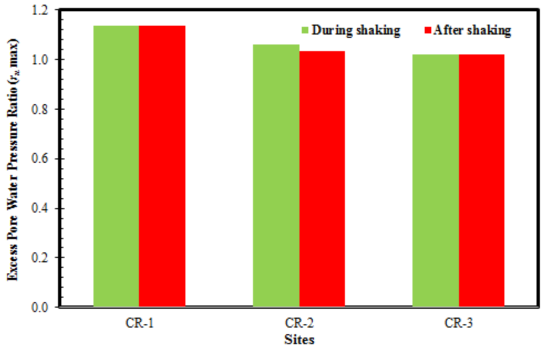

Fig 15a. Maximum excess pore water pressure ratio during and after shaking

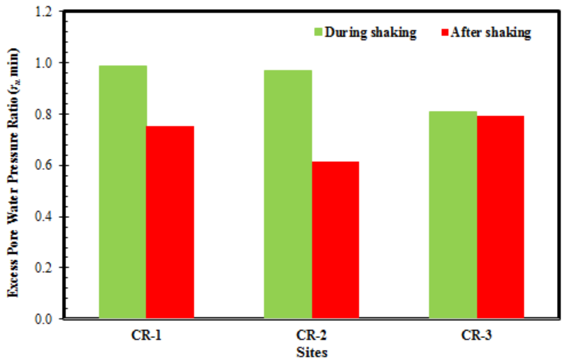

Fig 15b. Minimum excess pore water pressure ratio during and after shaking

(4) Liquefaction duration

Based on time history of excess pore water pressure on each liquefiable layer, the duration of liquefaction is calculated, as shown in Table 2. Table 2 presents the duration of liquefaction for the liquefiable layer in overall. It can be seen from Table 2 that CR-3 provides the longest duration than other sites, i.e. for 50 seconds, whereas the shortest duration is provided by CR-1. The liquefaction duration is obviously effected by the velocity of excess pore water pressure to build up. In Chiang Rai site, the liquefiable soils are dominated by sandy layer with soil type of SP-SM.

Table 2 liquefaction duration on liquefiable layer

Site	Liquefaction Duration (s)	
	Maximum	Minimum
CR-1	40	0
CR-2	43	39
CR-3	50	39

This soil type has the lower resistance of SPT. The lower resistance usually provides the lower shear stress and tends to be more contractive. When the excess pore water pressure builds up, and reaches or passes the initial effective stress, it will be concentrated at liquefied point during shaking. Even after shaking, the remained energy of wave propagation still contributes to keep the excess pore water pressure concentrating at threshold point.

(5) Percentage of total r_u on overall sand layers and impacted depth

Table 3 presents the percentage of excess pore water pressure ratio resulted in all sand layers. In Table 3, excess pore water pressure ration distribution is divided into 7 groups. From Table 3, it can be seen that excess pore water pressure ratio varies in all sites. In general, it can be concluded that in overall soil column, CR-3 and CR-2 undergo worse impacted depth than CR-1. The impacted depth due to liquefaction on each site referring to percentage of excess pore water pressure ratio is compiled in Table 4

Table 3 Percentage of r_u in sand layer.

Total r_u in overall sand layer (%)	Sites		
	CR-1	CR-2	CR-3
$r_u \geq 1$	8.77	38.33	32.79
$0.9 < r_u < 1$	5.26	18.33	19.67
$0.8 < r_u < 0.9$	5.26	0.00	1.64
$0.7 < r_u < 0.8$	3.51	0.00	6.56
$0.6 < r_u < 0.7$	5.26	0.00	8.20
$0.6 < r_u < 0.5$	3.51	0.00	13.11
$r_u < 0.5$	68.42	43.33	18.03

Table 4 Impacted depth based on r_u.

Impacted depth (m)	Sites		
	CR-1	CR-2	CR-3
$r_u \geq 1$	2.54	11.31	9.84
$0.9 < r_u < 1$	1.53	5.41	5.90
$0.8 < r_u < 0.9$	1.53	0.00	0.49
$0.7 < r_u < 0.8$	1.02	0.00	1.97
$0.6 < r_u < 0.7$	1.53	0.00	2.46
$0.6 < r_u < 0.5$	1.02	0.00	3.93
$r_u < 0.5$	19.84	12.78	5.41

In Table 4, it can be seen that total of impacted depth due to liquefaction ($r_u \geq 1$) is intensively found on Chiang Rai site. The impacted depth is from 2.5 to 11.3 m deep. However, the attention also must be concerned for impacted depth due to $0.9 < r_u < 1$. If an earthquake with the bigger magnitude and PGA attacks those depths, the excess pore water pressure ratio might be higher. If this condition happens, the impacted depth will become larger.

4. CONCLUDING REMARKS

This study focuses on non-linear finite element simulation of soil liquefaction due to 24 March 2011 earthquake or Tarlay earthquake. Several analyses, such as seismic response analysis, excess pore water pressure analysis, soil behaviour under existing earthquake loading, and etc. are conducted in this study. The following conclusions are drawn from this study:

1. Due to Tarlay earthquake 2011, Northern Thailand experienced the heavy damage and catastrophic hazard, such as liquefaction. Liquefaction was found in shallow depth, as reported by some researchers. In this study, the analysis result also shows that liquefaction is vulnerable on shallow depth, which is indicated by the excess pore water pressure ratio more than or equal to 1. Moreover, the liquefaction also results in the settlement, which is predicted about 4 to 1.8 cm at ground surface. It indicates that there is soil compressibility of liquefiable layer due to earthquake shaking, as result of liquefaction phenomenon. However, to estimate the detail observation during earthquake, the physical model, such as 1g model or scaled model (centrifuge test) test should be conducted.
2. The maximum and minimum excess pore water pressure ratios during and after earthquake are also observed. The result indicates that the excess pore water pressure ratio is not easily drained, so the value of excess pore water pressure ration during and after earthquake is almost the same. The further analysis also shows that minimum excess pore water pressure ratio in liquefiable soil is generated at the deeper depth, otherwise the maximum excess pore water pressure ratio is generated at the shallower depth. The result also indicates that the bottom-up pressure of excess pore water give the contribution to keep the pore water pressure concentrating at shallow depth. In addition, the effect of free vibration after shaking, still produces a little excess pore water pressure due to propagated wave energy. This continuous effect seems also to contribute in decreasing the effective stress at shallow depth. Therefore, the excess pore water pressure ratio keeps higher during and after earthquake. In the next study, excess pore water pressure and dissipated pore water pressure in long term will be conducted to observe the final pore water pressure distribution. It is also interesting to conduct the effect of aftershock study through to the produced excess pore water pressure ratio.
3. The liquefaction duration during earthquake shaking shows that for SP and SM with lower SPT value soil layer undergoes the longer duration of liquefaction. As explained in the previous points, the existence of fines content and bottom-up pressure of pore water pressure play role in determining the liquefaction duration. In addition, the liquefiable layer indicated to undergo liquefaction is also calculated. In general, it can be shown that the impacted depth is at shallow depth. This gives the prediction for the actual earthquake shaking in Northern Thailand. However, the attention also must be paid to the higher earthquake magnitude and PGA. Since higher magnitude and PGA may be possible to produce worse impacted depth than this study. According to excess pore pressure ratio interpretation, the excess pore water pressure close to 1 is also found on the depth below the impacted depth. This depth is very vulnerable to be liquefied when the stronger earthquake happens. By referring to the result of impacted depth prediction in Northern Thailand. The soil improvement for the shallow depth and foundation design should be concerned in Northern Thailand.
4. Cyclic ratio and cyclic shear strain are also reflected to excess pore water pressure ratio. Based on their interpretations, it can be found that, there are several factor influencing the excess pore water pressure ratio, such as fines content of soil type, and effective confining pressure. To strengthen this result, an experimental study in laboratory should be conducted. However, this study has given a little clue in determining the liquefaction threshold of cyclic shear strain triggering liquefaction.

ACKNOWLEDGEMENT: The authors would like to thank Dr. Suttisak Soralump for providing relevant data and useful suggestions throughout the research. The authors would be grateful for the financial support from the AUN/SEED-net (JICA).

REFERENCES

1) Ruangrassamee A, Ornthammarat T, and Lukkunaprasit P. : Damage due to 24 March 2011 M6.8 Tarlay Earthquake in Northern Thailand, *Proceeding of 15th World Conference of Earthquake Engineering (WCEE), Lisboa, Portugal*, 2012.
2) Soralump S, Feungaugsorn J. : Probabilistic analysis of liquefaction potential "the first eyewitness case in Thailand, *Proceeding of 18th National Convention of Civil Engi-*

neering (NCCE), Chiang Mai, Thailand, 2013.

3) Tanapalungkorn W, Teachavorasinskun S. : Liquefaction susceptibility due to earthquake in Northern Parts of Thailand, *Proceeding of the 20th National Convention of Civil Engineering (NCCE)*, Chonburi, Thailand, 2015.
4) Mase, L.Z, Likitlersuang, S, Soralump S, and Tobita T. : Empirical study of liquefaction potential in Chiang Rai Province in the North of Thailand, Proceeding of 28th conference of Kyoto University-Korean Advance Institute of Science and Technology-Hongkong University of Science and Technology-Tongji University-Chulalongkorn University-National Taiwan University, and National University of Singapore (KKHTCNN), Bangkok, Thailand, 2015.
5) National Earthquake Hazards Reduction Program (NEHRP). : Recommended Provisions for Seismic Regulation for New Buildings and Other Structures, 1997 Edition, Part 1 – Provisions, Part 2 – Commentary, FEMA 302, 1998.
6) Thai Meteorological Department (TMD). : Seismological Bureau (Earthquake Data of 2011 Earthquake), Thai Meteorological Department, 2015.
7) Elgamal A, Yang Z, Lu J. : Cyclic 1D : A computer program of seismic ground response, Department of Structural Engineering, University of California, San Diego, La Jolla. California, USA Report No. SSRP-06/05, 2006.
8) Pender M.J., Orense R.P., Wotherspoon L.M., and Storie L.B. : Effect of permeability on cyclic generation and dissipation of pore pressure in saturated gravel layers, *J. Geothechnique*., Vol.66, No.4, pp.313-322., 2016. DOI: 10.1680/jgeot.SIP.15.P.024.
9) Ishihara K, Tatsuoka F, and Yasuda, S. : Undrained deformation and liquefaction of sand under cyclic stresses, *J. Soils and Foundation*. Vol.15, No.1, pp.29–44, 1975.
10) Elgamal A, Yang Z, Parra E, and Ragheb A. : Modeling of cyclic mobility in saturated cohesionless soils, *Int. J. Plasticity*, Vol.19, No.6, pp.883-905, 2003.
11) Parra E. : Numerical modeling of liquefaction and lateral ground deformation including cyclic mobility and dilation response in soil system, PhD Thesis, Department of Civil Engineering, Rensselaer Polytechnic Institute, Troy. New York, USA, 1996.
12) Yang Z. : Numerical modeling of earthquake site response including dilation and liquefaction, PhD Dissertation, Department of Civil Engineering and Engineering Mechanics, Columbia University. New York, USA, 2000.
13) Prevost, J.H. : A simple plasticity theory for frictional cohesionless soils, *J. Soil Dynamics and Earthquake Engineering*, Vol.4, No.1, pp.9-17, 1985.
14) Elgamal Z, Yang Z, Parra E. : Computational modelling of cyclic mobility and post liquefaction site response, J. *Soil Dynamics and Earthquake Engineering*, Vol.22, No.4, pp.259-271, 2002.
15) Yang Z, Elgamal A. Influence of permeability on liquefaction induces shear deformation, *J. Engineering Mechanics*, ASCE, Vol.128, No.7, pp.720-729, 2002.
16) Yang Z, Elgamal A, Parra J. : Computational model for cyclic mobility and associated shear deformation, *J. Geotechnical and Enviromental Engineering*, ASCE, Vol.129, No.12, pp.1119-1127, 2003.
17) Yang Z, Lu J, Elgamal A. : A web-based platform for computer simulation of seismic ground response, *J. Advances in Engineering Software*, Vol.35, No.5, pp.249-259, 2004.